

## Virtual Restoration of Cracks in Murals Based on Maximum Entropy Thresholding and Planar Structure Information

Pengyu Sun<sup>1,2</sup>, Miaole Hou<sup>1,2</sup>, Zhensong Zhang<sup>3</sup>, Haishi Duan<sup>3</sup>, Shuqiang Lyu<sup>1,2</sup>

<sup>1</sup> Beijing University of Civil Engineering and Architecture, No.15 Yongyuan Road, Daxing District, Beijing 102616, China - 1108140023001@stu.bucea.edu.cn, houliaole@bucea.edu.cn, lvshuqiang@bucea.edu.cn

<sup>2</sup> Beijing Key Laboratory for Architectural Heritage Fine Reconstruction & Health Monitoring, No.15 Yongyuan Road, Daxing District, Beijing, China - 1108140023001@stu.bucea.edu.cn, houliaole@bucea.edu.cn, lvshuqiang@bucea.edu.cn

<sup>3</sup> Beijing Art Museum (Wanshou Temple), Beijing, China - 1942636637@qq.com, 2858824609@qq.com

**Keywords:** Virtual restoration, Mural, Cracks, Maximum Entropy Threshold, Planar Structural Information.

### Abstract

Ancient murals, as invaluable cultural heritage, carry profound historical and cultural significance. However, they are often subjected to environmental factors such as temperature fluctuations, humidity, and seismic activity, which frequently result in the formation of surface cracks. This study proposes an image processing-based approach for the digital conservation of murals, introducing a method that integrates maximum entropy thresholding with planar structure information to virtually restore crack degradation in high-resolution mural images. The proposed technique comprises two main stages: crack extraction and restoration. Crack regions are identified using a combination of bottom-hat transformation, maximum entropy thresholding, connected component labeling, and mathematical morphology. Following extraction, a planar structure information algorithm is applied to restore the affected areas. By leveraging the inherent planar characteristics and structural regularities of mural images, these features are incorporated as constraints within the PatchMatch algorithm to improve restoration results. The approach has been successfully applied to real mural cases. Compared to existing techniques, it not only produces superior visual outcomes but also shows clear advantages in quantitative metrics such as SSIM, PSNR, and AGD. This virtual restoration method effectively and authentically eliminates cracks in high-resolution mural images, providing valuable guidance for practical restoration efforts while preserving the integrity and artistic essence of the murals. Thus, it contributes to the advancement of high-definition digital conservation and the long-term protection of cultural heritage.

### 1. Introduction

Murals are cultural heritage treasures with enormous historical, social, and artistic value. As a unique form of artistic expression, colorful and unique murals are an important source of artistic creation and inspiration for our descendants. Unfortunately, due to long-term effects such as temperature, humidity, earthquakes, and weathering, the majority of murals have suffered varying degrees of damage, resulting in the appearance of cracks on their surfaces, which compromises the visual aesthetics and integrity of the murals(Wang et al., 2023). These fragile murals therefore need to be preserved and restored.

The traditional method for repairing cracks in traditional murals includes surface cleaning, filling materials, smoothing, and adjusting color and texture(Liu et al., 2021). However, due to the delicate nature of mural surfaces, this restoration method presents certain challenges. The murals are susceptible to further damage if errors occur during the restoration procedure. The image-based virtual restoration technology achieves non-contact restoration of cultural relics and provides effective strategies for manual restoration. In recent years, image-based virtual restoration techniques have demonstrated tremendous potential in mural preservation. Virtual restoration techniques can digitally record and preserve the original appearance of murals, reducing physical contact and minimizing the risk of further damage(Hou et al., 2018; Sun et al., 2023). This helps protect the integrity and value of the murals. Additionally, virtual restoration allows murals to be showcased in a digital format, transcending geographical and temporal limitations(Del Mastio, 2007). This enables a larger audience to appreciate, learn, and study murals, greatly facilitating the sharing and inheritance of cultural heritage.

In the field of mural restoration research based on traditional image processing techniques, Mol and colleagues (Mol et al.,

2021) employed an extended-exemplar-based region filling algorithm with the aim of virtually restoring deteriorated murals. They also utilized a patch-based reconstruction procedure and implemented a dynamic mask generation algorithm to automatically create mask images for the identification of damaged areas and subsequent pixel value analysis for restoration. Furthermore, Poornapushpakala and fellow researchers (Poornapushpakala et al., 2022) conducted preprocessing on images of Tanjore paintings using Wiener filtering, aimed at eliminating background noise. Subsequently, they applied the processed images to an inpainting algorithm for the digitization and preservation of these artworks. In addition, Cao and colleagues (Cao et al., 2019) introduced the ASB-LS algorithm, which is based on the Criminisi algorithm and is specifically focused on addressing flaking damage in the Kaihua Temple murals from the Song Dynasty. This algorithm involves an analysis of the mural's compositional characteristics, the introduction of a structure tensor to redefine data items for precise structural preservation, and the improvement of image filling order through the incorporation of a novel data item-based priority function. They also implemented a local search strategy to enhance matching efficiency. However, current research based on traditional image processing techniques predominantly emphasizes issues related to mural degradation, with relatively limited discussions pertaining to linear pathologies such as cracks.

Advances in the fields of computer vision and deep learning have led to the increasing utilization of various neural networks for the virtual restoration of murals. Zhou et al. (Zhou et al., 2022) introduced an innovative approach to restoration based on deep learning and structural guidance. Through a structure-guided feature optimization module, this method explicitly leverages the inherent color relationships within structural information to select pertinent features for enhancing the quality of color restoration in missing areas of Dunhuang mural images. The

results show a significant improvement in restoring the color quality of missing structural regions in Dunhuang mural images. Lyu et al. (Lv et al., 2022) have introduced an innovative network architecture specifically crafted for the segregation of contour and content pixels within mural images. Initially, a contour restoration generator network is employed, which integrates skip connections and layered residual blocks for contour repair. Subsequently, guided by the restored contours, a content completion network is utilized to restore the colored mural images. Xu et al. (Xu et al., 2023) have proposed a digital restoration method that combines Deformable Convolution (DCN), ECANet, ResNet, and Cycle Generative Adversarial Network (CycleGAN). This method, referred to as DC-CycleGAN, offers superior inpainting results and enhanced model performance for color restoration in Dunhuang mural images. Presently, deep learning-based mural restoration methods have exhibited remarkable performance in terms of restoration quality, yet they also present certain limitations. Much of the research is confined to murals of a specific style, such as those found in Dunhuang. Additionally, the size and resolution of the mural to be restored impose specific requirements, making it challenging to support high-resolution, high-definition mural images.

In conclusion, the study of automated digital mural image restoration technology is of significant importance. Advancing this technology not only directly contributes to the conservation of frescoes and enhances operational efficiency, but also fosters broader developments in image processing techniques. Due to the unique characteristics of murals, few reference images are available for restoration. Consequently, image restoration typically relies on existing known information to infer the missing parts. However, the complex patterns inherent in murals are often severely disrupted by crack deterioration, which increases the challenges of restoration. Crack degradation in murals frequently appears as extensive areas of fine and elongated forms, making crack repair particularly challenging and necessitating innovative and effective restoration methods. In this study, a combined approach integrating maximum entropy thresholding with plane-structure-guided methods is utilized to achieve virtual crack restoration in murals. A sequence of processes including bottom-hat transformation, maximum entropy thresholding, connected component labeling, and mathematical morphological operations is developed for automatic crack extraction and mask generation. For crack restoration, a plane-structure-guided approach is adopted, incorporating planarity and regularity detection as constraints in the objective function of the PatchMatch algorithm. Additionally, the exhaustive search in the original sample-based restoration algorithm is replaced by the Approximate Nearest Neighbour (ANN) method, which introduces a directed search strategy into the image patch matching process, thereby enabling the retrieval of optimal matching patches for filling the missing regions. Importantly, this method is not limited by the size or style of mural images and can be applied to the restoration of high-resolution, large-scale murals, providing a path towards high-precision digital preservation.

## 2. Materials and methods

### 2.1 Materials

The mural samples utilized in this study originate from Wanshou Temple and Qutan Temple, each exhibiting its distinctive artistic style. According to historical records, the murals at both temples date back to the Ming Dynasty. Despite multiple restorations over the centuries, the current condition of the murals remains

unsatisfactory, with numerous large cracks compromising their original integrity and decorative quality. The murals were photographed using a Nikon D850 DSLR camera equipped with an 80 mm lens. Images were acquired at a spatial resolution of  $8256 \times 5504$  pixels, with the camera ISO set to 100. LED lights with a color temperature of 5500 K were employed as external light sources. Due to the characteristics of the camera, light intensity, and ambient light color, images may not accurately reproduce the subject's true appearance. To address this, Adobe Lightroom Classic CC software was used to perform color correction on the original digital images captured in Nikon Electronic Format, using the ColorChecker Passport MSCCPP-B as the reference color card. This process ensured accurate reproduction of the mural's tones as perceived by the human eye. Figure 1 illustrates the comprehensive workflow of the proposed method for mural crack restoration.

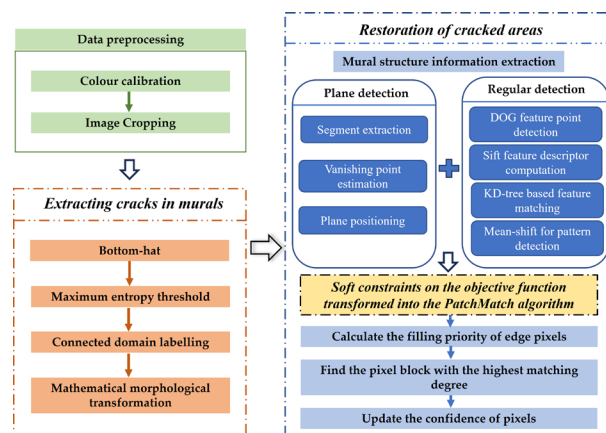


Figure 1. Overall workflow of the proposed method.

### 2.2 Crack extraction based on maximum entropy thresholding

Previous observations indicate that crack degradation in murals typically exhibits two characteristics: a darker color and an elongated shape. The bottom-hat morphological operation, which detects valleys in an image, is particularly suitable for processing images with bright backgrounds and dark features. Therefore, a bottom-hat transformation was first applied to enhance the visibility of cracks, facilitating subsequent extraction steps.

The maximum entropy thresholding method assumes that the crack and background regions follow distinct probability distributions separated by a threshold. After applying a bottom-hat transformation, crack areas exhibit higher intensity values than the background. The method computes the information entropy of both regions based on the histogram and defines the total entropy as their sum. The optimal threshold is the one that maximizes this total entropy, effectively distinguishing crack regions from the background (Kapur et al., 1985).

The maximum entropy threshold segmentation can roughly extract the crack region, but it also includes some noise points and non-fracture regions. To improve the accuracy of the fracture area extraction, connected domain labelling was used (Unnikrishnan et al., 1987). Each connected region was allowed to form an identified block by labelling the pixels extracted from the previous step, and the geometric information of these blocks was obtained. In this study, the area was chosen as the geometric information of the cracked area's connected domain marker. If

the connected domain's area was less than a specific threshold, the area was removed.

Following the previous steps, the cracked regions in the murals were extracted. However, discontinuities were observed in the extracted crack patterns. A closing operation was applied to fill small voids within the fracture zones and to connect adjacent fracture segments. To achieve optimal restoration results, a subsequent dilation operation was performed on the output of the closing process. This ensured that the cracked regions completely encompassed the corresponding areas in the original mural image, thereby generating an effective mask for the subsequent restoration phase.

### 2.3 Crack restoration guided by planar structure information

The planar structure information image complementation requires planar and regularity detection of mural images to be restored. This helps the best similar blocks to be matched and copied to the missing areas, achieving better recovery results (Huang et al., 2014).

Line segment extraction, vanishing point estimation, and planar localization techniques were used to achieve the planar detection of mural images. First, edges and fitted line segments were detected in the known areas of the mural image to be restored. The RANSAC-based Voting Approach detects up to three vanishing points, assuming that there are at most three different planar orientations in the image. Finally, by pairing the three detected vanishing points, three different planar orientations could be recovered, thereby completing the planar detection of the mural image (Yuhang et al., 2016).

The next step was to perform regularity detection on the mural images. The scale-invariant feature transform operator was computed for each feature point after detecting the standard difference between Gaussian feature points in a known region of the mural image to be recovered. The two nearest neighbours of each feature were then computed using a K-dimensional tree. All feature matches with a high prior probability were extracted at two feature locations for each plane. The perspective distortion of repeated structures in 2D space was removed by an affine correction of the positions of the matching feature points. The mean-shift algorithm (Comaniciu et al., 2002) was used to detect repetitive translational patterns, where the objective function for recovering cracks in the mural image is shown in Equation (1).

$$\min_{\{t_i, s_i, m_i\}} \sum_{i \in \Omega} E_{color}(s_i, t_i, m_i) + E_{guide}(s_i, t_i, m_i),$$

$$E_{color}(s_i, t_i, m_i) = \|q(s_i, t_i, m_i) - p(t_i)\|, \quad (1)$$

$$E_{guide}(s_i, t_i, m_i) = \alpha_1 E_{plane}(s_i, t_i, m_i) + \alpha_2 E_{direction}(s_i, t_i, m_i) + \alpha_3 E_{proximity}(s_i, t_i),$$

where  $\Omega$  is the set of intact pixel indices of the mural image;  $\bar{\Omega}$  is the set of pixel indices of the cracked area of the mural image;  $t_i$  is the centre of the target block in  $\bar{\Omega}$ ;  $s_i$  is the centre of the corresponding source block in  $\Omega$ ;  $m_i$  is the plane index of  $t_i$ ;  $E_{color}$  is the colour term of the mural image;  $E_{guide}$  is the plane information term;  $E_{plane}$  is the plane compatibility term;  $E_{direction}$  is the orthogonal direction term;  $E_{proximity}$  is the proximity term. The equations for the plane compatible term,

orthogonal direction term, and proximity term are shown in (2).

$$E_{plane}(s_i, t_i, m_i) = -\log Pr[m_i|s_i] - \log Pr[m_i|t_i],$$

$$E_{direction}(s_i, t_i, m_i) = \Psi(\min(|H_{m_i}^1(\tilde{s}_i)^y - H_{m_i}^1(\tilde{t}_i)^y|, |H_{m_i}^2(\tilde{s}_i)^y - H_{m_i}^2(\tilde{t}_i)^y|))$$

$$H_{m_i}^j = \begin{bmatrix} \cos \theta_j & -\sin \theta_j & 0 \\ \sin \theta_j & \cos \theta_j & 0 \\ l_1^{m_i} & l_2^{m_i} & l_3^{m_i} \end{bmatrix}, \quad (2)$$

$$E_{proximity}(s_i, t_i) = \frac{\|s_i - t_i\|_2^2}{\sigma_d(t_i)^2 + \sigma_c^2}, \quad \sigma_c^2 = (W/8)^2,$$

where  $Pr[m_i|s_i]$  is the posterior probability map;  $Pr[m_i|t_i]$  is the planar affiliation of the assignment located at  $s_i, t_i$ ;  $\Psi(z) = \min(|z|, c)$  is the function that restricts the cost to a constant  $c = 0.02$ ;  $H_{m_i}^j$  is the definition of the mapping;  $\sigma_d(t_i)^2$  is the target location squared distance from the boundary of the nearest known region;  $\sigma_c^2$  is the parameter that adjusts the strength of the neighbourhood cost;  $W$  is the maximum image size.

By identifying multiple planes present in the image and detecting corresponding translational patterns, defining prior probabilities for block offsets and transformations, the planar structure information is transformed into soft constraints of the objective function to achieve PatchMatch image repair.

The principle of the PatchMatch repair algorithm is to change the brute-force search method used in traditional sample-based repair algorithms to ANN. This introduces a directed search strategy for the process of matching image patches, enhancing the efficiency of the search. Additionally, during the reconstruction process, a set of more intuitive repair interaction controls are proposed. These controls can be used to constrain the entire local repair process, leading to improved repair results. The repair principle of the PatchMatch algorithm is illustrated in Figure 2(a), where  $\Omega$  represents the target region to be repaired, and  $\Phi$  represents the non-missing parts outside the target region (Songtao et al., 2021). The repair process of this algorithm primarily consists of three steps:

Step 1: Calculate the filling priority of edge pixels. Let  $\delta\Omega$  be the boundary between the known region and the damaged region. Let  $q$  be the center point of the candidate region within the known region. Let  $p$  be the pixel with the highest current priority value, and  $\Psi p$  be the region centered around point  $p$ .  $\nabla I_p^\perp$  represents the direction of the iso-intensity line at point  $p$ ,  $n_p$  is the unit normal vector perpendicular to the boundary at point  $p$ , and  $9 \times 9$  is the default patch size. The priority calculation formula for the priority value  $P(p)$  of point  $p$  is as follows:

$$P(p) = C(p) \times D(p), \quad (3)$$

In the equation, the calculation of the confidence term  $C(p)$  and the gradient data term  $D(p)$  is as follows:

$$\frac{C(p) = \sum_{q \in \Psi p \cap \Omega} C(p) / |\Psi p|}{D(p) = |\nabla I_p^\perp \cdot n_p| / \alpha} \quad (4)$$

During the initialization, if  $\forall p \in \Omega, C(p) = 0, \forall p \notin \Omega,$

$C(p) = 1$ . In the equation,  $|\Psi p|$  represents the number of pixels in the sample block,  $\alpha$  is the normalization factor. A higher value of  $C(p)$  indicates that there is more complete information surrounding point  $p$ , indicating a higher confidence level. Therefore, areas with higher confidence should be prioritized for restoration.

Step 2: Perform ANN global search to find the pixel block with the highest matching degree. ANN is divided into initialization and iterative computation parts. During the initialization process, as shown in Figure 2(b), a random candidate's nearest neighbor can be assigned to each block to be matched, either randomly or based on specific prior knowledge. According to the Law of Large Numbers, it is possible to find at least one block  $(x, y)$  for which the candidate's nearest neighbor area  $f(x, y)$  is its true nearest neighbor area. An iterative computation process begins after the initialization step, starting from block  $(x, y)$ . This process mainly includes two steps: first, there is a propagation process, where the nearest neighbor of the block  $(x_0, y_0)$  is calculated through its adjacent blocks that already have known nearest neighbors. To ensure the accuracy of this calculation, a random search process is added after the propagation process. This process randomly selects a block within a gradually decreasing window to calculate its distance to the block to be matched, stopping when the window size is smaller than the size of the block. Therefore, the size of the search area decreases exponentially, as shown in Equation (5). Afterward, the closest distance and the corresponding block found during the entire computation process are taken as the approximate nearest neighbor of the block to be matched. Finally, repeat the propagation process and random search until the number of iterations is reached. ANN leverages the continuity of images to reduce the search range significantly and ensures that most points converge as quickly as possible through iteration. This dramatically reduces unnecessary calculations and improves processing efficiency.

$$u_i = v_0 + \omega \alpha^i R_i, \quad (5)$$

Of these,  $v_0 = f(x, y)$ ,  $R_i$  is a uniformly distributed random point within  $[-1, 1] \times [-1, 1]$ ,  $\omega$  is the maximum search radius,  $\alpha$  is the search radius decay rate.

Let  $\Psi p$  be the sample block with the highest priority, and  $\Psi q$  be a sample block in the intact region of the image. The optimal matching block should satisfy the following equation (Yongwei et al., 2018):

$$\Psi q = \arg \min(SSD(\Psi p, \Psi q)), \quad (6)$$

In the equation,  $SSD(\Psi p, \Psi q)$  represents the sum of squared differences between the corresponding pixel colors within the two sample blocks. Once the optimal matching block  $\Psi q$  is found through the search, the pixel information from  $\Psi q$  is then filled into the corresponding positions of the missing region in  $\Psi p$ .

Step 3: Update the confidence of pixels in the  $\Psi p$  block. After repairing a module, the previously unknown region within that module becomes a known region. As a result, the confidence within the module will change. The updating method for confidence is as follows:

$$C(p) = C(q), \quad (7)$$

In the equation,  $p \in (\Psi p \cap \Omega)$  indicates that the process is repeated until the damaged region is completely repaired. The point  $p$  represents an edge point that needs to be repaired, and the point  $q$  represents a point in the known region. If the repair region is filled with content from the known region, the confidence of point  $p$  and point  $q$  will be equal and updated accordingly.

The structural information of the mural image was extracted and translated into constraints on the objective function of the PatchMatch repair algorithm. As a result, the optimal similar blocks could be matched and copied to the defective region, and the repair of the unknown region could be completed step by step. Beginning with the intact area of the mural image, the blocks that were most similar to the cracked area were matched and filled into the broken cracked area. The cracked region in the mural was gradually repaired after several iterations.

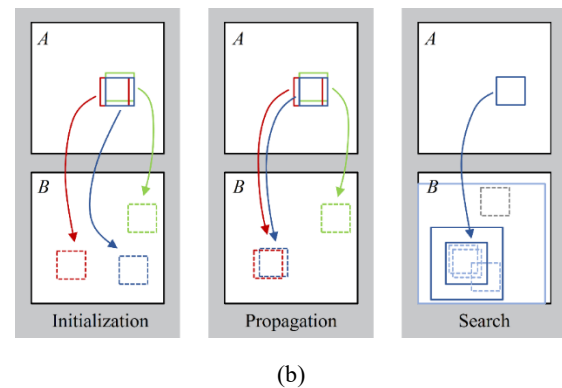
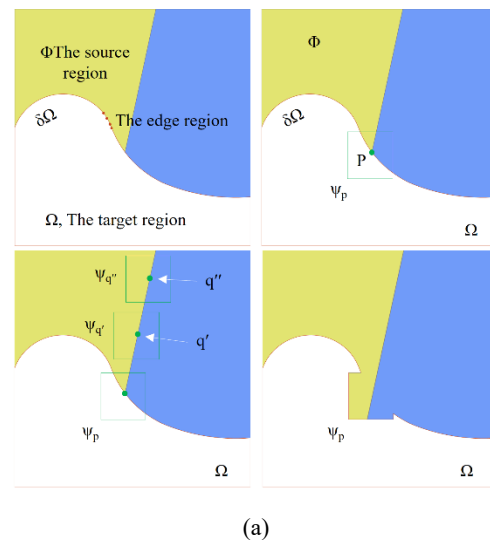


Figure 2. Inpainting schematic diagram based on PatchMatch. (a) is a schematic diagram of the repair principle of the PatchMatch algorithm and (b) is an illustration of the approximate nearest neighbor (ANN) computation process.

### 3. Results and discussion

To validate the effectiveness of the proposed method for crack restoration in mural images, this study conducted simulation experiments using Matlab2020b on a computer with a 3.20 GHz processor and 16 GB of memory. To accurately repair the crack region, a mask of the crack region should be obtained. The mask is then added to the original image to obtain the image to be repaired.



### 3.1 Crack extraction

The crack extraction results are shown in Figure 3. The first column presents the results after bottom-hat transformation. Based on the width of the mural cracks, a structuring element with a radius of 4 was selected, effectively enhancing the visibility of cracks and distinguishing them from the background. The second column shows the results of maximum entropy thresholding. To refine the extraction, connected component labeling was applied, as shown in the third column. An area threshold was used to filter small components, with values ranging from 5 to 60 compared. A threshold of 25 achieved the best balance, removing noise without losing fine cracks. The fourth column displays the results after applying closing and dilation operations to improve crack continuity. These steps helped fill gaps and expand the crack regions, preparing them for virtual restoration. The optimal structuring element sizes for closing and dilation were 6 and 4, respectively.

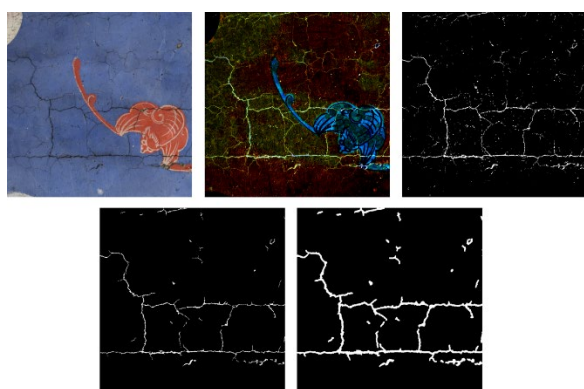


Figure 3. Crack extraction results.

### 3.2 Comparison of crack repair in actual murals

In this study, the aforementioned methods are applied to restore cracked degradation in murals of different styles and the results are shown in Figure 4. The restoration effects of various algorithms are shown as follows: (a) Restoration effect of the algorithm in the literature (Shen et al., 2002), (b) Restoration effect of the algorithm in the literature (Criminisi et al., 2004), (c) Restoration effect of the algorithm in the literature (Guo, 2021), (d) Restoration effect of LaMa, (e) Restoration effect of CoordFill, and (f) Restoration effect of the algorithm proposed in this study. It can be observed that the crack areas repaired using the literature (Shen et al., 2002) is inconsistent with the background region, resulting in noticeable blurring. The literature (Criminisi et al., 2004) has a problem with some areas being filled in incorrectly. Restoring with the literature (Guo, 2021) leads to a decrease in mural clarity, while LaMa and CoordFill exhibit overall satisfactory performance, albeit with still unsatisfactory details. Compared to other methods, the recommended approach demonstrates superior visual effects, achieving a more natural and clear transition between the restored crack areas and the background region.

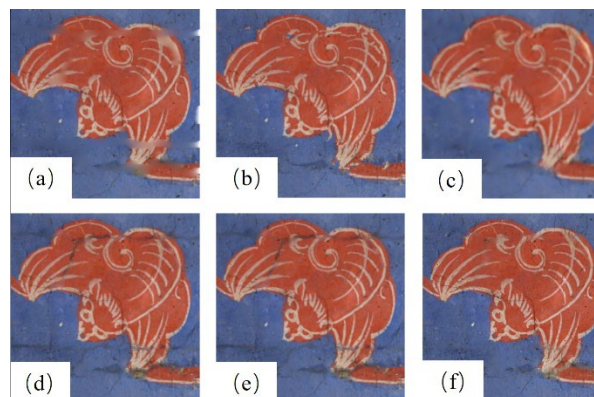


Figure 4. Comparison of different algorithms.

### 3.3 Objective analysis

To objectively evaluate the restoration results, we selected Structural Similarity Index (SSIM), Peak Signal-to-Noise Ratio (PSNR), and Average Gradient Difference (AGD) as objective assessment metrics. The SSIM value reflects the correlation of structural information before and after mural restoration. By comparing the contrast, structure, and brightness of the restored image with the ground truth image, it reflects the similarity between the two images. A higher value indicates better restoration results. PSNR is used to judge the restoration effect by calculating the signal error between the restored image and the ground truth image. A higher PSNR value indicates better restoration results. AG evaluates the edge strength or texture complexity of the image, and a higher AG value usually indicates that the image has more edge and texture details, representing higher image clarity. By deducting the AG value of the repaired image using different techniques from that of the original image, we can obtain a more precise evaluation of the restoration quality achieved by diverse methods, which we define as AGD. The restoration effect is better when the AGD value is smaller. This is because the restored image becomes closer to the original image in terms of clarity.

Since SSIM and PSNR are reference-based evaluation metrics, the crack-free mural was selected as the ground truth, as shown in Figure 5(a). As shown in Figure 5(b), simulated crack degradation was applied to these murals, which was used for calculating the evaluation indices. The comparison results of different methods (enlarged views) are shown in Figure 6. Figure 6 shows the restoration effects produced by different algorithms: (a) the method proposed by (Shen et al., 2002), (b) the method of (Criminisi et al., 2004), (c) the method of (Guo, 2021), (d) LaMa, (e) CoordFill, and (f) the algorithm proposed in this study. It is evident that the method proposed by (Shen et al., 2002) performs significantly in restoring visible cracks, but the restored areas appear somewhat blurry. The results from (Criminisi et al., 2004) reveal filling errors in certain regions, and the restoration traces are clearly noticeable. Although the GAN-based network (Guo, 2021) achieves favorable results in some areas, it does not support high-resolution mural restoration. Moreover, the output of the GAN network is compressed to  $512 \times 512$  pixels, leading to a reduction in mural clarity, which is clearly reflected in the AGD metric.

In contrast, high-resolution networks such as LaMa and CoordFill focus more on the overall visual perception after restoration. However, for murals as artistic pieces, the restoration of fine details is of greater importance. As shown in Table 1, these methods still slightly underperform the approach proposed in this

study in terms of SSIM, PSNR, and AGD. The AG value of the reference image is 4.6340.

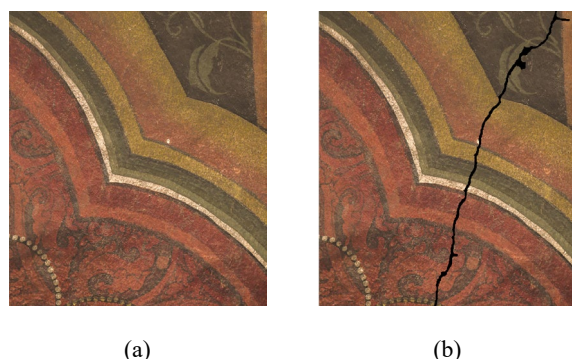


Figure 5. (a) The original mural image, (b) artificially damaged mural image.

#### 4. Conclusion

The study aims to present an automated approach that incorporates a maximum entropy thresholding and planar structure information algorithm to extract and repair cracks in mural images. A range of methods, including bottom-hat transformation, maximum entropy thresholding, connected component labelling, and mathematical morphology, are employed to identify and extract cracks from murals. Additionally, planar structure information is integrated to constrain the PatchMatch algorithm, thereby improving the accuracy of virtual restoration. Through experiments conducted on multiple high-resolution images of cracked murals with varying styles, it was demonstrated that the proposed technique can effectively restore a significant portion of crack areas, resulting in more refined and complete mural images that closely reproduce the original appearance. However, when mural patterns are complex, crack extraction results remain suboptimal. Moreover, inconsistencies persist in repairing line patterns when the crack areas are large. Further research is necessary to improve the algorithm. In future work, digital restoration techniques will be investigated to address various degradation problems observed in ancient murals, thereby enabling the virtual restoration of multiple types of deterioration.

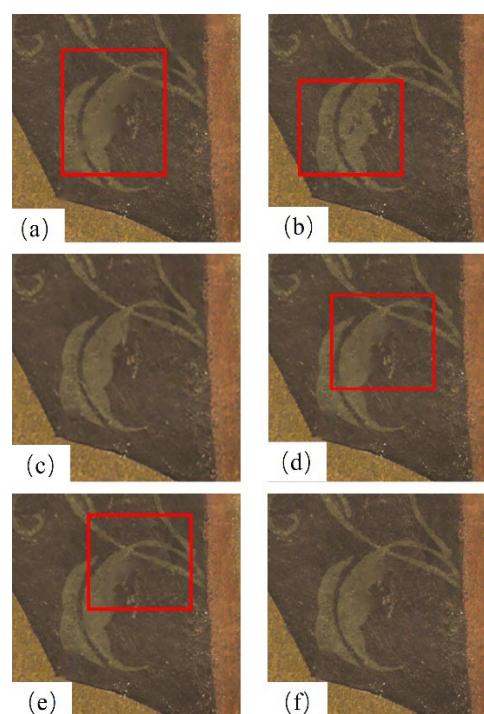


Figure 6. Comparison of the local magnifications of the repair effects of different algorithms on artificial destruction.

Methods	SSIM	PSNR	AGD
Literature (Shen et al., 2002)	0.9987	98.3731	0.2627
Literature (Criminisi et al., 2004)	0.9977	93.8087	0.0603
Literature (Guo, 2021)	0.9985	81.7956	2.4796
LaMa	0.9972	95.7451	1.5623
CoordFill	0.9972	95.7851	1.5587
Proposed method	0.9992	105.4356	0.1265

Table 1. Evaluation metrics after restoration by different algorithms.

#### References

- Cao, J., Y. Li, Q. Zhang, and H. Cui. 2019. Restoration of an ancient temple mural by a local search algorithm of an adaptive sample block. *Heritage Science* 7:39. doi: 10.1186/s40494-019-0281-y.
- Comaniciu, D., and P. Meer. 2002. Mean shift: A robust approach toward feature space analysis. *IEEE Transactions on Pattern Analysis and Machine Intelligence* 24:603-619. doi: 10.1109/34.1000236.
- Criminisi, A., P. Perez, and K. Toyama. 2004. Region filling and object removal by exemplar-based image inpainting. *IEEE*

- Transactions on Image Processing* 13:1200-1212. doi: 10.1109/TIP.2004.833105.
- Del Mastio, A., V. Cappellini, R. Caldelli, A. De Rosa, and A. Piva. 2007. Virtual restoration and protection of cultural heritage images, in 2007 15th International Conference on Digital Signal Processing, 471-474: IEEE.
- Guo, X., H. Yang, and D. Huang. 2021. Image inpainting via conditional texture and structure dual generation, in 2021 IEEE/CVF International Conference on Computer Vision (ICCV), 14114-14123.
- Hou, M., P. Zhou, S. Lv, Y. Hu, X. Zhao, W. Wu, H. He, S. Li, and L. Tan. 2018. Virtual restoration of stains on ancient paintings with maximum noise fraction transformation based on the hyperspectral imaging. *Journal of Cultural Heritage* 34:136-144. doi: <https://doi.org/10.1016/j.culher.2018.04.004>.
- Huang, J.-B., S. B. Kang, N. Ahuja, and J. Kopf. 2014. Image completion using planar structure guidance. *ACM Trans. Graph.* 33:Article 129. doi: 10.1145/2601097.2601205.
- Jianmin, L., W. Qi, L. Zhenrong, and Y. Liang. 2018. Improved cdd image inpainting model algorithm. *Computer Engineering and Design* 39:2564-2569. doi: 10.16208/j.issn1000-7024.2018.08.029.
- Juhui, Q. 2020. Image inpainting method based on image partition and improved criminisi algorithm. *Modern Electronics Technique* 43:63-66. doi: 10.16652/j.issn.1004-373x.2020.01.017.
- Kapur, J. N., P. K. Sahoo, and A. K. C. Wong. 1985. A new method for gray-level picture thresholding using the entropy of the histogram. *Computer Vision, Graphics, and Image Processing* 29:273-285. doi: [https://doi.org/10.1016/0734-189X\(85\)90125-2](https://doi.org/10.1016/0734-189X(85)90125-2).
- Liu, C., Y. He, Q. Li, and F. Wang. 2021. Study on the causes of secondary cracks of the cave wall mural of daxiong hall at fengguo temple in yixian, liaoning, china. *Heritage Science* 9:127. doi: 10.1186/s40494-021-00601-5.
- Lv, C., Z. Li, Y. Shen, J. Li, and J. Zheng. 2022. Separafill: Two generators connected mural image restoration based on generative adversarial network with skip connect. *Heritage Science* 10:135. doi: 10.1186/s40494-022-00771-w.
- Mol, V. R., and P. U. Maheswari. 2021. The digital reconstruction of degraded ancient temple murals using dynamic mask generation and an extended exemplar-based region-filling algorithm. *Heritage Science* 9:137. doi: 10.1186/s40494-021-00604-2.
- Poornapushpakala, S., S. Barani, M. Subramoniam, and T. Vijayashree. 2022. Restoration of tanjore paintings using segmentation and in-painting techniques. *Heritage Science* 10:41. doi: 10.1186/s40494-022-00661-1.
- Shen, J., and T. F. Chan. 2002. Mathematical models for local nontexture inpaintings. *SIAM Journal on Applied Mathematics* 62:1019-1043. doi: 10.1137/s0036139900368844.
- Songtao, L., L. Weigang, S. Jingrui, and G. Ping. 2021. Inpainting of metallographic image based on improved patchmatch algorithm. *Metal heat treatment* 46:196-205. doi: 10.13251/j.issn.0254-6051.2021.03.039.
- Sun, X., J. Jia, P. Xu, J. Ni, W. Shi, and B. Li. 2023. Structure-guided virtual restoration for defective silk cultural relics. *Journal of Cultural Heritage* 62:78-89. doi: <https://doi.org/10.1016/j.culher.2023.05.016>.
- Unnikrishnan, A., Y. V. Venkatesh, and P. Shankar. 1987. Connected component labelling using quadrees – a bottom-up approach. *The Computer Journal* 30:176-182. doi: 10.1093/comjnl/30.2.176.
- Wang, Y., and X. Wu. 2023. Current progress on murals: Distribution, conservation and utilization. *Heritage Science* 11:61. doi: 10.1186/s40494-023-00904-9.
- Xu, Z., C. Zhang, and Y. Wu. 2023. Digital inpainting of mural images based on dc-cycleGAN. *Heritage Science* 11:169. doi: 10.1186/s40494-023-01015-1.
- Yongwei, M., L. Lili, W. Xun, Z. Xudong, and L. Zhen. 2018. Editing single flower image based on cone proxy. *Journal of Computer-Aided Design & Computer Graphics* 30:1466-1478. doi: 10.3724/sp.J.1089.2018.16779.
- Yuhang, M., L. Guangyao, and X. Mang. 2016. Image completion based on planar structure information. *Computer Engineering* 42:236-241,248. doi: 10.3969/j.issn.1000-3428.2016.03.043.
- Zhou, Z., X. Liu, J. Shang, J. Huang, Z. Li, and H. Jia. 2022. Inpainting digital dunhuang murals with structure-guided deep network. *Journal of Cultural Heritage*. 15:Article 77. doi: 10.1145/3532867.